

# ZEROFLOW: FAST, ZERO LABEL, SCALABLE SCENE FLOW VIA DISTILLATION

Kyle Vedder<sup>1\*</sup> Neehar Peri<sup>2</sup> Nathaniel Chodosh<sup>2</sup> Ishan Khatri<sup>3</sup> Eric Eaton<sup>1</sup>

Dinesh Jayaraman<sup>1</sup> Yang Liu Deva Ramanan<sup>2</sup> James Hays<sup>4</sup>

<sup>1</sup>University of Pennsylvania <sup>2</sup>Carnegie Mellon University <sup>3</sup>Motional <sup>4</sup>Georgia Tech

## ABSTRACT

Scene flow estimation is the task of describing the 3D motion field between temporally successive point clouds. State-of-the-art methods use strong priors and test-time optimization techniques, but require on the order of tens of seconds to process large-scale point clouds, making them unusable as computer vision primitives for real-time applications such as open world object detection. Feed forward methods are considerably faster, running on the order of tens to hundreds of milliseconds for large-scale point clouds, but require expensive human supervision. To address both limitations, we propose *Scene Flow via Distillation*, a simple, scalable distillation framework that uses a label-free optimization method to produce pseudo-labels to supervise a feed forward model. Our instantiation of this framework, *ZeroFlow*, achieves **state-of-the-art** performance on the *Argoverse 2 Self-Supervised Scene Flow Challenge* while using zero human labels by simply training on large-scale, diverse unlabeled data. At test-time, ZeroFlow is over  $1000\times$  faster than label-free state-of-the-art optimization-based methods on large-scale point clouds and over  $1000\times$  cheaper to train on unlabeled data compared to the cost of human annotation of that data. To facilitate further research, we will release our code, trained model weights, and high quality pseudo-labels for the Argoverse 2 and Waymo Open datasets.

## 1 INTRODUCTION

Scene flow estimation is an important primitive for open-world object detection and tracking (Najibi et al., 2022; Zhai et al., 2020; Baur et al., 2021; Huang et al., 2022; Erçelik et al., 2022). For example, Najibi et al. (2022) generates supervisory boxes for an open-world LiDAR detector via offline object extraction using high quality scene flow estimates from Neural Scene Flow Prior (NSFP) (Li et al., 2021b). Although NSFP does not require human supervision, it takes tens of seconds to run on a single large-scale point cloud pair. If NSFP were both high quality and fast enough to run in real-time, its estimations could be directly used as a runtime primitive in the downstream detector, instead of being relegated to an offline pipeline. This runtime feature formulation is similar to Zhai et al. (2020)’s use of scene flow from FlowNet3D (Liu et al., 2019) as an input primitive for their multi-object tracking pipeline; although FlowNet3D is fast enough for online processing of modestly-sized point clouds, its supervised feed forward formulation requires significant in-domain human annotations.

Broadly, these exemplar methods are representative of the strengths and weakness of their class of approach: state-of-the-art scene flow methods train feed forward models using *extremely expensive* human annotations<sup>1</sup>, or use test-time optimization techniques that operate without human annotations, but are too slow for online scene flow estimation<sup>2</sup>.

We propose *Scene Flow via Distillation* (SFvD), a framework that, while conceptually simple, generates a new class of scene flow estimation methods that combine the strengths of optimization-

\*Corresponding email: [kvedder@seas.upenn.edu](mailto:kvedder@seas.upenn.edu)

<sup>1</sup>At  $\sim \$0.10$  / cuboid / frame, the Argoverse 2 (Wilson et al., 2021) *train* split cost  $\sim \$750,000$  to label; ZeroFlow’s pseudo-labels cost  $\$394$  at current cloud compute prices. See Supplemental D for details.

<sup>2</sup>Neural Scene Flow Prior (Li et al., 2021b) takes more than 26 seconds per point cloud pair on the Argoverse 2 (Wilson et al., 2021) *train* split. See Supplemental D for details.

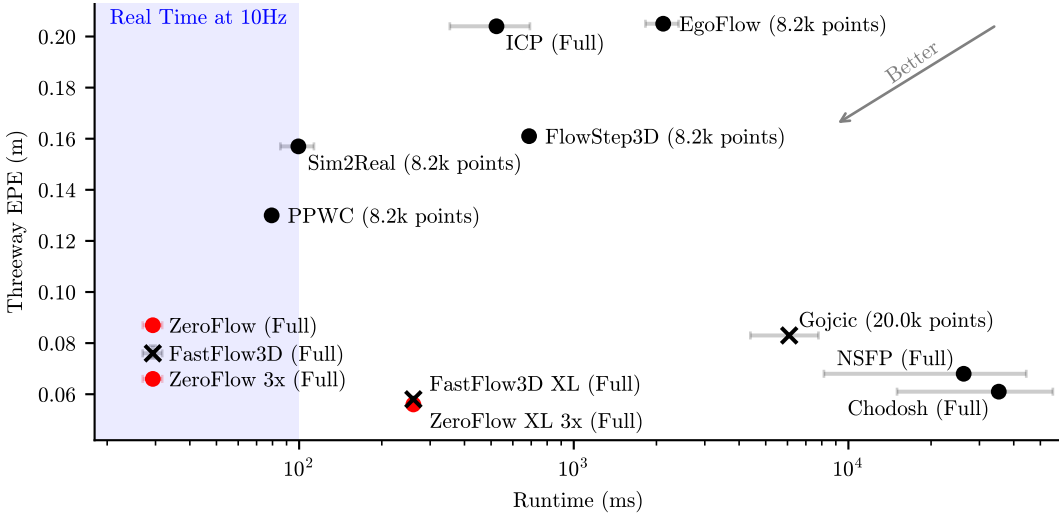


Figure 1: We plot the performance and run-time of recent scene flow methods on the Argoverse 2 Sensor dataset (Wilson et al., 2021), along with the size of the point cloud prescribed in the method’s evaluation protocol. Our method **ZeroFlow 3X** outperforms its teacher (NSFP, Li et al. (2021b)) while running over  $1000\times$  faster, and **ZeroFlow XL 3X** captures **state-of-the-art**. Methods that use *any* human labels are plotted with  $\times$ , and zero-label methods are plotted with  $\bullet$ .

based and feed forward methods with the power of data scale (Sutton, 2019) to achieve fast run-time and high accuracy without human supervision. We instantiate this pipeline into *Zero-Label Scalable Scene Flow* (ZeroFlow), a family of methods that can process large-scale point clouds while providing high quality scene flow estimates. We demonstrate the strength of ZeroFlow on Argoverse 2 Wilson et al. (2021) and Waymo Open Sun et al. (2020), notably achieving **state-of-the-art** on the *Argoverse 2 Self-Supervised Scene Flow Challenge* by simply using a larger student network and training on additional unlabeled data from the Argoverse 2 LiDAR dataset (Figure 1).

Our primary contributions include:

- We introduce a simple yet effective distillation framework, *Scene Flow via Distillation* (SFvD), which uses a label-free optimization method to produce pseudo-labels to supervise a feed forward model, allowing us to achieve or even surpass the performance of slow optimization-based approaches at the speed of feed forward methods.
- Using SFvD, we present *Zero-Label Scalable Scene Flow* (ZeroFlow), a family of methods that produce fast, **state-of-the-art** scene flow on large-scale clouds, running over  $1000\times$  faster than state-of-the-art optimization methods on real point clouds, while being over  $1000\times$  cheaper to train compared to the cost of human annotations.
- We release high quality flow pseudo-labels (representing 7.1 GPU months of compute) for the popular Argoverse 2 (Wilson et al., 2021) and Waymo Open (Sun et al., 2020) autonomous vehicle datasets, alongside our code and trained model weights, to facilitate research reuse.

## 2 BACKGROUND AND RELATED WORK

Given point clouds  $P_t$  at time  $t$  and  $P_{t+1}$  at time  $t+1$ , scene flow estimators predict  $\hat{F}_{t,t+1}$ , a 3D vector for each point in  $P_t$  that describes how it moved from  $t$  to  $t+1$  (Dewan et al., 2016). Performance is traditionally measured using the Endpoint Error (EPE) between the predicted flow  $\hat{F}_{t,t+1}$  and ground truth flow  $F_{t,t+1}^*$  (Equation 1):

$$\text{EPE}(P_t) = \frac{1}{\|P_t\|} \sum_{p \in P_t} \left\| \hat{F}_{t,t+1}(p) - F_{t,t+1}^*(p) \right\|_2. \quad (1)$$

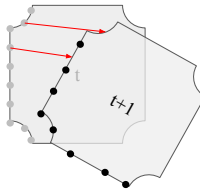


Figure 2: Scene Flow vectors describe where the point on an object at time  $t$  will end up on the object at  $t + 1$ . In this example, the upper ground truth flow vector, associated with a point in the upper left concave corner of the object at  $t$  has no nearby observations at  $t + 1$  due to occlusion of the concave feature. Additionally, the lower ground truth flow vector, associated with a point on the face of the object at  $t$ , does not directly match with a point on the object at  $t + 1$  due to sparsity of the observational points on the object face.

Unlike next token prediction in language (Radford et al., 2018) or next frame prediction in vision (Weng et al., 2021), future observations do not directly provide the ground truth flow (Figure 2); instead, ground truth must be provided by human annotation or a synthetic dataset’s generator.

To get around this limitation, recent approaches to scene flow either acquire their priors via supervision from human annotations (Liu et al., 2019; Behl et al., 2019; Tishchenko et al., 2020; Kittenplon et al., 2021; Wu et al., 2020; Puy et al., 2020; Li et al., 2021a; Jund et al., 2021; Gu et al., 2019; Battrawy et al., 2022; Wang et al., 2022), via human-designed test-time surrogate objective optimization over hand-designed representations (Pontes et al., 2020; Eisenberger et al., 2020; Li et al., 2021b; Chodosh et al., 2023), or via self-supervision from human-designed surrogate objectives (Mittal et al., 2020; Baur et al., 2021; Gojcic et al., 2021; Dong et al., 2022; Li et al., 2022). Supervised methods are efficient at test-time; however, they require costly human annotations at train-time. Both test-time optimization and self-supervised methods seek to address this problem through the use of label-free surrogate objectives such as Chamfer distance (Pontes et al., 2020), cycle-consistency (Mittal et al., 2020), and various hand-designed rigidity priors (Dewan et al., 2016; Pontes et al., 2020; Li et al., 2022; Chodosh et al., 2023; Baur et al., 2021; Gojcic et al., 2021). Self-supervised methods achieve faster inference by forgoing expensive test-time optimization, but do not match the quality of optimization-based methods (Chodosh et al., 2023) and tend to require human-designed priors via more sophisticated network architectures compared to supervised methods (Baur et al., 2021; Gojcic et al., 2021; Kittenplon et al., 2021); in practice, this makes them slower and more difficult to train.

### 3 METHOD

We propose *Scene Flow via Distillation* (SFvD), a conceptually simple distillation framework which describes a new class of scene flow estimation methods that are fast, high quality, and require zero human supervision (Figure 3). Concretely, we use a label-free optimization-based method to generate scene flow pseudo-labels, which are used to supervise a fast feed forward model. While conceptually simple, efficiently instantiating SFvD requires careful construction; most online optimization methods and feed forward models are unable to efficiently scale to large-scale point clouds (Section 3.1).

Based on our scalability analysis, we propose a family of scene flow methods *Zero-Label Scalable Scene Flow* (ZeroFlow) based on SFvD that produces fast, **state-of-the-art** scene flow estimates for full size point clouds without any human labels (Algorithm 1). ZeroFlow uses Neural Scene Flow prior (NSFP) (Li et al., 2021b) to generate high quality, label-free pseudo-labels on full-size point clouds (Section 3.2) and a feed forward architecture from the FastFlow3D (Jund et al., 2021) family for efficient flow inference (Section 3.3).

#### 3.1 SCALING SCENE FLOW VIA DISTILLATION TO LARGE POINT CLOUDS

Popular AV datasets including Argoverse 2 (Wilson et al., 2021) (collected with dual Velodyne VLP-32 sensors) and Waymo Open (Sun et al., 2020) (collected with a proprietary lidar sensor and subsampled) have large-scale point clouds with an average of 52,000 and 79,000 points per frame, respectively, after ground plane removal (Supplemental A and Figure 6). For practical applications, sensors such as the Velodyne VLP-128 in dual return mode produce up to 480,000 points per

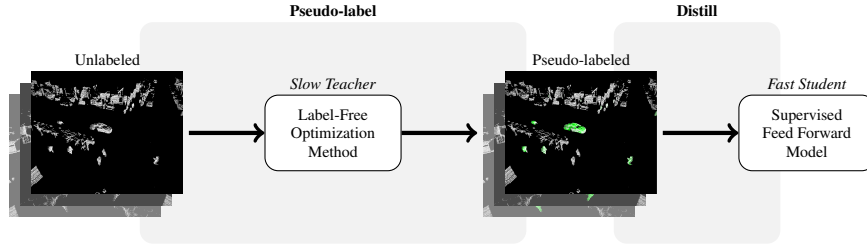


Figure 3: The *Scene Flow via Distillation* (SFvD) framework, which describes a new class of scene flow methods that produce high quality, human label-free flow at the speed of feed forward networks.

sweep (Vel, 2019) and proprietary sensors at full resolution can produce well over 1 million points per sweep. Thus, scene flow methods must scale to large-scale point clouds for real-world applications.

Unfortunately, most methods focus strictly on scene flow *quality* for toy point clouds constructed by randomly subsampling full point clouds down to 8,192 points (Jin et al., 2022; Tishchenko et al., 2020; Wu et al., 2020; Kittenplon et al., 2021; Liu et al., 2019; Li et al., 2021b). Motivated by real-world applications, we target scene flow estimation for the full point cloud. At this scale, architectural efficiency is of paramount importance. FastFlow3D (Jund et al., 2021), which uses a PointPillar-style (Lang et al., 2019) encoder, can process 1 million points in under 100 ms on an NVIDIA Tesla P1000 GPU (making it real-time for a 10Hz lidar), while methods like FlowNet3D (Liu et al., 2019), which use 3D point-wise convolutions, take almost 4 seconds to process the same point cloud.

We design our approach to effectively scale to large point clouds. For SFvD’s pseudo-labeling step, method run-time is less of a concern — pseudo-labeling each point cloud pair is embarrassingly parallel, and high-quality methods like Neural Scene Flow Prior (NSFP) (Li et al., 2021b) require only a modest amount of GPU memory (under 3GB) when estimating scene flow on point clouds with 70K points. This enables fast pseudo-labeling using commodity GPUs; as described in Supplemental D, pseudo-labeling the Argoverse 2 train split with NSFP is over 1000 $\times$  cheaper than human annotation. The runtime of SFvD’s student feed forward model is critical, as it determines the method’s test-time speed, motivating models that can efficiently process large-scale point clouds.

### 3.2 NEURAL SCENE FLOW PRIOR IS A SLOW TEACHER

Neural Scene Flow Prior (NSFP) (Li et al., 2021b) is an optimization-based approach to scene flow estimation. Notably, it does not use ground truth labels to generate high quality flows, instead relying upon strong priors from its learnable function class (determined by the architecture of its coordinate network) and proxy measures of scene flow (e.g. Equation 2). Point residuals are fit per point cloud pair  $P_t, P_{t+1}$  at runtime by randomly initializing two MLPs; one to describe the forward flow  $\hat{F}^+$  from  $P_t$  to  $P_{t+1}$ , and one to describe the reverse flow  $\hat{F}^-$  from  $P_t + \hat{F}_{t,t+1}$  to  $P_t$  in order to impose a cyclic constraint. The forward flow  $\hat{F}^+$  and backward flow  $\hat{F}^-$  are then optimized jointly to minimize

$$\text{TruncatedChamfer}(P_t + \hat{F}^+, P_{t+1}) + \text{TruncatedChamfer}(P_t + \hat{F}^+ + \hat{F}^-, P_t) , \quad (2)$$

where TruncatedChamfer is the standard Chamfer distance with per-point distances above 2 meters set to zero to reduce the influence of outliers.

NSFP is able to produce high-quality scene flow estimations due to its choice of coordinate network architecture and cyclical constraint. The coordinate network’s learnable function class is expressive enough to fit the low frequency signal of residuals for moving objects while restrictive enough to avoid fitting the high frequency noise from TruncatedChamfer, and the cyclic constraint acts as a smoothness regularizer for the forward flow. NSFP provides high quality estimates on full size point clouds (Figure 1), making it a good candidate for the pseudo-label step of SFvD.

### 3.3 FASTFLOW3D IS A FAST STUDENT

FastFlow3D (Jund et al., 2021) is an efficient feed forward network that learns using human supervisory labels  $F_{t,t+1}^*$  and per-point foreground / background class labels. FastFlow3D minimizes a

variation of the End-Point Error (Equation 1) that reduces the importance of background points, thus minimizing

$$\frac{1}{\|P_t\|} \sum_{p \in P_t} \sigma(p) \left\| \hat{F}_{t,t+1}(p) - F_{t,t+1}^*(p) \right\|_2 \quad (3) \quad \text{where} \quad \sigma(p) = \begin{cases} 1 & \text{if } p \in \text{Foreground} \\ 0.1 & \text{if } p \in \text{Background} \end{cases} \quad (4)$$

FastFlow3D uses a PointPillars-style encoder (Lang et al., 2019), traditionally used for efficient LiDAR object detection (Vedder & Eaton, 2022), with a U-Net style backbone. The encoder of the U-Net processes  $P_t$  and  $P_{t+1}$  separately, and the decoder jointly processes both embeddings. A small MLP is used to extract scene flow for each point in  $P_t$  using the point’s coordinates and its associated output pillar feature.

As discussed in Section 3.1, FastFlow3D’s design choices make it highly scalable for large point clouds. While most feed forward networks are evaluated on a standard toy evaluation protocol with subsampled point clouds, FastFlow3D is able to scale up to full resolution point clouds while maintaining real-time performance and emitting competitive quality scene flow estimates, making it a good candidate for the distillation step of SFvD.

In order to train FastFlow3D using pseudo-labels, we replace the foreground / background scaling function (Equation 4) with a simple uniform weighting ( $\sigma(\cdot) = 1$ ); see Supplemental B for experiments with other weighting schemes. Additionally, we depart from FastFlow3D’s problem setup in two minor ways. Unlike FastFlow3D, we delete ground points using dataset provided maps, and use the standard scene flow problem setup of predicting residuals (Section 2) instead of predicting future flow vectors in meters per second given two prior frames. Our approach is given in Algorithm 1, with setup details specified in Section 4.1.

In order to take advantage of the unlabeled data scaling of SFvD, we expand FastFlow3D to a family of models by designing a higher capacity backbone, producing *FastFlow3D XL*. This larger backbone halves the size of each pillar to quadruple the pseudoimage area, doubles the size of the pillar embedding, and adds an additional layer to maintain the network’s receptive field in metric space; as a result, the total parameter count increases from 6.8 million to 110 million.

---

**Algorithm 1** ZeroFlow
 

---

```

1:  $D \leftarrow$  collection of unlabeled point cloud pairs ▷ Training Data
2: for  $P_t, P_{t+1} \in D$  do ▷ Embarrassingly Parallel For
3:    $F_{t,t+1}^* \leftarrow \text{TeacherNSFP}(P_t, P_{t+1})$  ▷ SFvD Pseudo-label Step
4: for epoch  $\in$  epochs do ▷ SFvD’s Distill Step
5:   for  $P_t, P_{t+1}, F_{t,t+1}^* \in D$  do
6:      $l \leftarrow$  Equation 3(StudentFastFlow3D $_{\theta}(P_t, P_{t+1}), F_{t,t+1}^*)$ 
7:      $\theta \leftarrow \theta$  updated w.r.t.  $l$ 
  
```

---

## 4 EXPERIMENTS

ZeroFlow is designed to provide a family of fast, high quality scene flow estimators. In order to validate this family and understand the impact of components in the underlying Scene Flow via Distillation framework, we perform extensive experiments on the Argoverse 2 (Wilson et al., 2021) and Waymo Open (Sun et al., 2020) datasets. We compare to first party implementations of NSFP (Li et al., 2021b) and Chodosh et al. (2023), implement FastFlow3D (Jund et al., 2021) ourselves (no first party implementation is available), and use Chodosh et al. (2023)’s implementations for all other baselines.

As discussed in Chodosh et al. (2023), downstream applications typically rely on good quality scene flow estimates for foreground points. Most scene flow methods are evaluated using average Endpoint Error (EPE, Equation 1); however, roughly 80% of real-world point clouds are background, causing average EPE to be dominated by background point performance. To address this, we use the improved

evaluation metric proposed by Chodosh et al. (2023), *Threeway EPE*:

$$\text{Threeway EPE}(P_t) = \text{Avg} \begin{cases} \text{EPE}(p \in P_t : p \in \text{Background}) & (\text{Static BG}) \\ \text{EPE}(p \in P_t : p \in \text{Foreground} \wedge F_{t,t+1}^*(p) \leq 0.5\text{m/s}) & (\text{Static FG}) \\ \text{EPE}(p \in P_t : p \in \text{Foreground} \wedge F_{t,t+1}^*(p) > 0.5\text{m/s}) & (\text{Dynamic FG}) \end{cases} . \quad (5)$$

#### 4.1 HOW DOES ZEROFLOW PERFORM VERSUS PRIOR ART ON REAL POINT CLOUDS?

The overarching promise of ZeroFlow is the ability to build fast, high quality scene flow estimators that improve with the the availability of *unlabeled* data. Does ZeroFlow deliver on this promise? How does it compare to state-of-the-art methods?

To characterize the ZeroFlow family’s performance, we use Argoverse 2 to perform scaling experiments along two axes: dataset size and student size. For our standard size configuration, we use the Argoverse 2 Sensor *train* split and the standard FastFlow3D architecture, enabling head-to-head comparisons against the fully supervised FastFlow3D as well as other baseline methods. For our scaled up dataset (denoted *3X* in all experiments), we use the Argoverse 2 Sensor *train* split and concatenate a roughly twice as large set of unsupervised frame pairs from the Argoverse 2 LiDAR dataset, drawn at a fixed interval across its 20,000 sequences to maximize data diversity. For our scaled up student architecture (denoted *XL* in all experiments), we use the *XL* backbone described in Section 3.3. For details on the exact dataset construction and method hyperparameters, see Supplemental A

Table 1: Quantitative results on the Argoverse 2 Sensor validation split using the evaluation protocol from Chodosh et al. (2023). The methods used in this paper, shown in the first two blocks of the table, are trained and evaluated on point clouds within a  $102.4\text{m} \times 102.4\text{m}$  area centered around the ego vehicle. However, following the protocol of Chodosh et al. (2023), all methods report error on points in the  $70\text{m} \times 70\text{m}$  area centered around the ego vehicle. Runtimes are collected on an NVIDIA V100 with a batch size of 1 (Li et al., 2020; Peri et al., 2023). FastFlow3D, ZeroFlow 1X, and ZeroFlow 3X have identical feed forward architectures and thus share the same real-time performance; FastFlow3D XL, ZeroFlow XL 1X, and ZeroFlow XL 3X have identical feed forward architectures and thus share the same performance. Methods with an \* have performance averaged over 3 training runs (see Supplemental C for details). Underlined methods require human supervision.

	Runtime (ms)		Point Cloud Subsample Size	Threeway EPE	Dynamic FG EPE	Static FG EPE	Static BG EPE	Dynamic AccRelax	Dynamic AccStrict
FastFlow3D* (Jund et al., 2021)			Full Point Cloud	0.076	0.186	0.021	0.021	0.474	0.200
ZeroFlow 1X* (Ours)	29.33 $\pm$	2.38	Full Point Cloud	0.092	0.231	0.022	0.022	0.380	0.150
ZeroFlow 3X (Ours)			Full Point Cloud	<b>0.066</b>	0.164	0.017	0.017	0.490	0.207
FastFlow3D XL			Full Point Cloud	0.058	0.139	0.018	0.018	0.585	0.276
ZeroFlow XL 1X (Ours)	260.61 $\pm$	1.21	Full Point Cloud	0.072	0.178	0.019	0.019	0.473	0.203
ZeroFlow XL 3X (Ours)			Full Point Cloud	<b>0.056</b>	0.131	0.018	0.018	0.595	0.305
NSFP w/ Motion Comp (Li et al., 2021b)	26, 285.0 $\pm$ 18, 139.3		Full Point Cloud	0.068	0.131	0.036	0.036	0.699	0.472
Chodosh et al. (Chodosh et al., 2023)	35, 281.4 $\pm$ 20, 247.7		Full Point Cloud	0.061	0.129	0.028	0.028	0.710	0.477
Odometry			Full Point Cloud	0.198	0.583	0.010	0.000	0.108	0.002
ICP (Chen & Medioni, 1992)	523.11 $\pm$	169.34	Full Point Cloud	0.204	0.557	0.025	0.028	0.112	0.015
Gojcic (Gojcic et al., 2021)	6, 087.87 $\pm$ 1, 690.56		20000	0.083	0.155	0.064	0.032	0.650	0.368
Sim2Real (Jin et al., 2022)	99.35 $\pm$	13.88	8192	0.157	0.229	0.106	0.137	0.565	0.254
EgoFlow (Tishchenko et al., 2020)	2, 116.34 $\pm$ 292.32		8192	0.205	0.447	0.079	0.090	0.111	0.018
PPWC (Wu et al., 2020)	79.43 $\pm$	2.20	8192	0.130	0.168	0.092	0.129	0.556	0.229
FlowStep3D (Kittenplon et al., 2021)	687.54 $\pm$	3.13	8192	0.161	0.173	0.132	0.176	0.553	0.248

As shown in Table 1, ZeroFlow is able to leverage scale to deliver superior performance. While ZeroFlow 1X loses a head-to-head competition against the human-supervised FastFlow3D, scaling the distillation process to additional unlabeled data enables ZeroFlow 3X to significantly surpass the performance of both methods just by using more raw data. Indeed, ZeroFlow 3X even surpasses the performance of its own teacher, NSFP, *while running in real-time!*

ZeroFlow’s pipeline also benefits from student scale. We scale up the student architecture with the much larger *XL* backbone, and show that our ZeroFlow *XL* 3X is able to combine the power of dataset and model scale to outperform all other methods, including significantly outperform its own teacher, and capture **state-of-the-art** on the Argoverse 2 validation split as well as the **first place on the Argoverse 2 Self-Supervised Scene Flow Challenge** hosted on the private Argoverse 2 test split.

To further validate ZeroFlow’s performance, we also train it on Waymo Open (Table 2), which lacks the same additional unlabeled point clouds available in Argoverse 2. As expected from the Argoverse 2 results, ZeroFlow 1X performs slightly worse than the human-supervised FastFlow3D.

Table 2: Quantitative results on Waymo Open using the evaluation protocol from Chodosh et al. (2023). Runtimes scaled to performance on a V100 (Li et al., 2020); both FastFlow3D and ZeroFlow 1X have identical feed forward architectures and thus share the same runtime. Underlined methods require human supervision.

	Runtime (ms)		Point Cloud Subsampled Size	Threeway EPE	Dynamic FG EPE	Static FG EPE	Static BG EPE	Dynamic AccRelax	Dynamic AccStrict
	21.66 $\pm$	0.48							
ZeroFlow 1X (Ours)	21.66 $\pm$	0.48	Full Point Cloud	0.083	0.216	0.016	0.017	0.376	0.149
FastFlow3D (Jund et al., 2021)	21.66 $\pm$	0.48	Full Point Cloud	0.075	0.195	0.015	0.016	0.490	0.239
Chodosh (Chodosh et al., 2023)	93,752.3 $\pm$	76,786.1	Full Point Cloud	<b>0.041</b>	0.073	0.013	0.039	0.877	0.726
NSFP Li et al. (2021b)	90,999.1 $\pm$	74,034.9	Full Point Cloud	0.100	0.171	0.022	0.108	0.539	0.331
ICP (Chen & Medioni, 1992)	302.70 $\pm$	157.61	Full Point Cloud	0.192	0.498	0.022	0.055	0.172	0.047
Gojcic Gojcic et al. (2021)	501.69 $\pm$	54.63	20000	0.059	0.107	0.045	0.025	0.844	0.584
EgoFlow (Tishchenko et al., 2020)	893.68 $\pm$	86.55	8192	0.183	0.390	0.069	0.089	0.178	0.046
Sim2Real (Jin et al., 2022)	72.84 $\pm$	14.79	8192	0.166	0.198	0.099	0.201	0.632	0.321
PPWC (Wu et al., 2020)	101.43 $\pm$	5.48	8192	0.132	0.180	0.075	0.142	0.497	0.217
FlowStep3D (Kittenplon et al., 2021)	872.02 $\pm$	6.24	8192	0.169	0.152	0.123	0.232	0.708	0.405

## 4.2 DOES ZEROFLOW’S PERFORMANCE FOLLOW PREDICTABLE SCALING LAWS?

Section 4.1 shows that ZeroFlow can leverage scale to capture state-of-the-art performance, but practitioners want to be able to estimate method performance from dataset size, in order to estimate their expected performance before launching a training run over their entire log history. Does ZeroFlow’s performance follow predictable scaling laws?

We train ZeroFlow and FastFlow3D on sequence subsets / supersets of the Argoverse 2 Sensor train split. Figure 4 shows ZeroFlow and FastFlow3D’s validation Threeway EPE both decrease roughly logarithmically, and this trend appears to hold for XL backbone models as well.

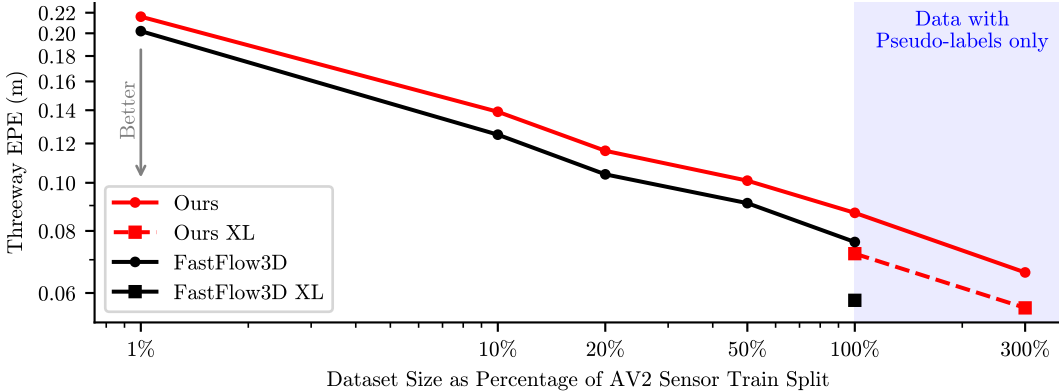


Figure 4: Empirical scaling law for ZeroFlow. Argoverse 2 validation split Threeway EPE as a percentage of the Argoverse 2 *train* split used, on a  $\log_{10}$ - $\log_{10}$  scale. Threeway EPE performance of ZeroFlow methods scales logarithmically with the amount of data.

## 4.3 HOW DOES DATASET DIVERSITY INFLUENCE ZEROFLOW’S PERFORMANCE?

In typical human annotation setups, an observational *sequence* is given to the human annotator. The human generates box annotations in the first frame, and then updates the pose of those boxes as the objects move through the sequence, introducing and removing annotations as needed. This process is much more efficient than annotating disjoint frame pairs, as it amortizes the time cost of setting up the box annotations for most objects in the sequence. This is why human annotated training datasets (e.g. Argoverse 2 Sensor, Waymo Open) are contiguous *sequences*. However, contiguous frames have significant structural similarity; in the 150 frames (15 seconds) of an Argoverse 2 Sensor sequence, the vehicle typically observes no more than a city block worth of unique structure.

ZeroFlow, which requires *zero* human labels, does not have this constraint on its pseudo-labels; NSFP run on sequential frames is just as expensive as NSFP run on non-sequential frames. Indeed for our high-performing 3X methods (Section 4.1), we concatenated onto the Argoverse 2 Sensor dataset a diverse subset of the Argoverse 2 LiDAR dataset built using 12 frame pairs selected at uniform

intervals selected from each of the 20,000 unique sequences to maximize scene diversity. How does dataset diversity impact ZeroFlow’s performance?

To understand the impact of data diversity, we train a version of ZeroFlow 1X and ZeroFlow 2X *only* on the diverse subset of our Argoverse 2 LiDAR data (Table 3). Unsurprisingly, dataset diversity has a non-trivial impact on performance; ZeroFlow 1X (AV2 LiDAR Subset Data) performs non-trivially better than ZeroFlow 1X trained on the contiguous sensor data, and ZeroFlow 2X (AV2 LiDAR Subset Data) matches the performance of the human supervised FastFlow3D.

Table 3: Comparison between ZeroFlow trained on Argoverse 2 Sensor dataset vs the more diverse, unlabeled Argoverse 2 LiDAR subset described in Section 4.1. Diverse training datasets result in non-trivial performance improvements.

	Threeway EPE	Dynamic FG EPE	Static FG EPE	Static BG EPE	Dynamic AccRelax	Dynamic AccStrict
FastFlow3D* (Jund et al., 2021)	0.076	0.186	0.021	0.021	0.474	0.200
ZeroFlow 1X (AV2 Sensor Data)*	0.092	0.231	0.022	0.022	0.380	0.150
ZeroFlow 1X (AV2 LiDAR Subset Data)	0.085	0.218	0.018	0.018	0.366	0.133
ZeroFlow 2X (AV2 LiDAR Subset Data)	0.076	0.184	0.022	0.022	0.449	0.188

#### 4.4 HOW DO THE NOISE CHARACTERISTICS OF ZEROFLOW COMPARE TO OTHER METHODS?

ZeroFlow uses Scene Flow via Distillation to distill NSFP into a feed-forward model from the FastFlow3D family. Section 4.1 highlights the *average* performance of ZeroFlow across Threeway EPE categories, but what does the error distribution look like?

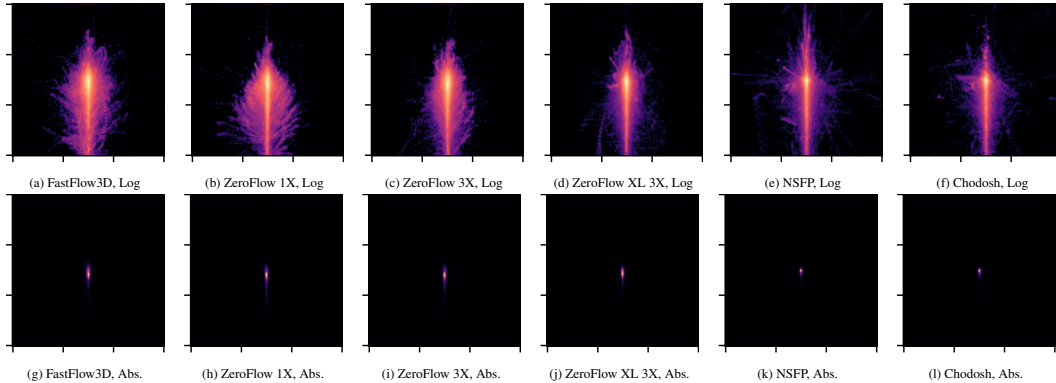


Figure 5: Normalized frame birds-eye-view heatmaps of endpoint residuals for Chamfer Distance, as well as the outputs for NSFP and Chodosh on moving points (points with ground truth speed above 0.5m/s). Perfect labels would produce a single central dot. Top row show the frequency on a  $\log_{10}$  color scale, bottom row shows the frequency on an absolute color scale. Qualitatively, methods with better quantitative results have tighter residual distributions.

To answer this question, we plot birds-eye-view flow vector residuals of NSFP, Chodosh, FastFlow3D, and several members of the ZeroFlow on moving objects from the Argoverse 2 validation dataset, where the ground truth is rotated vertically and centered at the origin to present all vectors in the same frame (Figure 5, see Supplemental E for details on construction).

Qualitatively, Figure 5 shows that distributional tightness ( $\log_{10}$  plots) roughly corresponds to overall method performance. ZeroFlow 1X has the worst overall performance, and this is reflected in both its  $\log_{10}$  plot (Figure 5b), which features residuals well below center, and the absolute scale plot (Figure 5h), which features a thin tail below center, caused by systematic underestimation of flow vector length. This distribution gets significantly tighter with ZeroFlow 3X (Figure 5c), which exceeds the performance of FastFlow3D and is reflected in its distributional tightness (Figure 5a). This trend is also seen in ZeroFlow 3X (Figure 5d), where its distribution roughly matches NSFP’s (Figure 5e), which has very similar Foreground Dynamic performance in Threeway EPE (Table 1);

note that ZeroFlow XL 3X significantly outperforms NSFP on the background buckets of Threeway EPE, resulting in a significantly improved overall Threeway EPE.

#### 4.5 HOW DOES TEACHER QUALITY IMPACT ZEROFLOW’S PERFORMANCE?

Section 4.1 compares NSFP (Li et al., 2021b) against Chodosh (Chodosh et al., 2023); Chodosh has superior Threeway EPE on both Argoverse 2 and Waymo Open. This raises the question: can a better performing teacher lead a better version of ZeroFlow?

To understand the impact of a better teacher, we train ZeroFlow on Argoverse 2 using superior quality flow vectors from Chodosh et al. (2023), which proposes a refinement step to NSFP labels to provide improvements to flow vector quality (Table 4). ZeroFlow trained on Chodosh refined pseudo-labels provides no meaningful quality improvement over the raw NSFP pseudo-labels (as discussed in Supplemental C, a Threeway EPE difference of 0.2cm is within training variance for ZeroFlow). These results also hold for our ablated speed scaled version of ZeroFlow in Supplemental B.

But pseudolabeling with NSFP is quite expensive; is it necessary? Can the commonly used self-supervised proxy of TruncatedChamfer be used as a pseudo-labeler to save computation expense?

To understand if NSFP is necessary, we train ZeroFlow on Argoverse 2 using pseudovectors from the nearest neighbor, truncated to 2 meters as with TruncatedChamfer. The residual distribution of TruncatedChamfer is shown in Supplemental E, Figure 9b. ZeroFlow trained on TruncatedChamfer pseudo-labels performs significantly worse than NSFP, motivating the use of NSFP as a pseudolabeler.

Table 4: Comparison between ZeroFlow trained on Argoverse 2 using NSFP pseudo-labels, ZeroFlow using Chodosh et al. (2023) pseudo-labels, and ZeroFlow using TruncatedChamfer. Methods with an \* have performance averaged over 3 training runs (see Supplemental C for details). The minor quality improvement of Chodosh pseudo-labels does not lead to a meaningful difference in performance, while the significant degradation of TruncatedChamfer leads to significantly worse performance.

	Threeway EPE	Dynamic FG EPE	Static FG EPE	Static BG EPE	Dynamic AccRelax	Dynamic AccStrict
ZeroFlow 1X (NSFP pseudo-labels)*	0.092	0.231	0.022	0.022	0.380	0.150
ZeroFlow 1X (Chodosh et al. (2023) pseudo-labels)	0.090	0.234	0.018	0.018	0.364	0.136
ZeroFlow 1X (TruncatedChamfer pseudo-labels)	0.108	0.226	0.049	0.049	0.411	0.153

## 5 CONCLUSION

Our scene flow approach, Zero-Label Scalable Scene Flow (ZeroFlow), produces fast, state-of-the-art scene flow *without human labels* via our conceptually simple distillation pipeline.

The human annotation free nature of our system provides several technical and social benefits. Due to the fact that human labels are *extremely expensive* to collect, sequences selected for annotation tend to be chosen for their *structural* diversity (e.g. dense urban scenes that tend to have lots of stationary objects) in order to maximally benefit LiDAR detectors. Our label-free training is orders of magnitude cheaper and is embarrassingly parallel, enabling a training run of the model on the *full* distribution of logs (including logs with significantly more motion but are uninteresting to LiDAR detectors, e.g. highways), thus directly matching the deployment distribution and consequently leading to greater robustness during deployment.

Breaking the dependence upon human annotations also democratizes scene flow — practitioners only need data and commodity GPUs to get labels, broadening the practical horizons for scene flow beyond domains with significant existing capital investments.

**Limitations and Future Work.** ZeroFlow inherits the biases of its pseudo-labels. Unsurprisingly, if the pseudo-labels consistently fail to predict scene flow for small objects, our method will also be unable to predict scene flow for these objects; however, further innovation in model architecture, loss functions, and pseudo-labels may yield better performance. In order to enable further work on Scene

Flow via Distillation-based methods, we release<sup>3</sup> our code, trained model weights, and NSFP flow pseudo-labels, representing 3.6 GPU months for Argoverse 2 and 3.5 GPU months for Waymo Open.

**Acknowledgements.** The research presented in this paper was partially supported by the DARPA SAIL-ON program under contract HR001120C0040, the DARPA ShELL program under agreement HR00112190133, the Army Research Office under MURI grant W911NF20-1-0080, and the CMU Center for Autonomous Vehicle Research.

## REFERENCES

Ramy Battrawy, René Schuster, Mohammad-Ali Nikouei Mahani, and Didier Stricker. RMS-FlowNet: Efficient and Robust Multi-Scale Scene Flow Estimation for Large-Scale Point Clouds. In *Int. Conf. Rob. Aut.*, pp. 883–889. IEEE, 2022.

Stefan Andreas Baur, David Josef Emmerichs, Frank Moosmann, Peter Pinggera, Björn Ommer, and Andreas Geiger. SLIM: Self-supervised LiDAR scene flow and motion segmentation. In *Int. Conf. Comput. Vis.*, pp. 13126–13136, 2021.

Aseem Behl, Despoina Paschalidou, Simon Donné, and Andreas Geiger. Pointflownet: Learning representations for rigid motion estimation from point clouds. In *Int. Conf. Comput. Vis.*, pp. 7962–7971, 2019.

Yang Chen and Gérard Medioni. Object modelling by registration of multiple range images. *Img. Vis. Comput.*, 10(3):145–155, 1992.

Nathaniel Chodosh, Deva Ramanan, and Simon Lucey. Re-Evaluating LiDAR Scene Flow for Autonomous Driving. *arXiv preprint*, 2023.

Ayush Dewan, Tim Caselitz, Gian Diego Tipaldi, and Wolfram Burgard. Rigid scene flow for 3d lidar scans. In *Int. Conf. Intel. Rob. Sys.*, pp. 1765–1770. IEEE, 2016.

Guanting Dong, Yueyi Zhang, Hanlin Li, Xiaoyan Sun, and Zhiwei Xiong. Exploiting Rigidity Constraints for LiDAR Scene Flow Estimation. In *IEEE Conf. Comput. Vis. Pattern Recog.*, pp. 12776–12785, 2022.

Marvin Eisenberger, Zorah Lahner, and Daniel Cremers. Smooth shells: Multi-scale shape registration with functional maps. In *IEEE Conf. Comput. Vis. Pattern Recog.*, pp. 12265–12274, 2020.

Emeç Erçelik, Ekim Yurtsever, Mingyu Liu, Zhijie Yang, Hanzhen Zhang, Pınar Topçam, Maximilian Listl, Yılmaz Kaan Çaylı, and Alois Knoll. 3D Object Detection with a Self-supervised Lidar Scene Flow Backbone. In Shai Avidan, Gabriel Brostow, Moustapha Cissé, Giovanni Maria Farinella, and Tal Hassner (eds.), *Computer Vision – ECCV 2022*, pp. 247–265, Cham, 2022. Springer Nature Switzerland.

Zan Gojcic, Or Litany, Andreas Wieser, Leonidas J Guibas, and Tolga Birdal. Weakly supervised learning of rigid 3d scene flow. In *IEEE Conf. Comput. Vis. Pattern Recog.*, pp. 5692–5703, 2021.

Xiuye Gu, Yijie Wang, Chongruo Wu, Yong Jae Lee, and Panqu Wang. Hplflownet: Hierarchical permutohedral lattice flownet for scene flow estimation on large-scale point clouds. In *IEEE Conf. Comput. Vis. Pattern Recog.*, pp. 3254–3263, 2019.

Shengyu Huang, Zan Gojcic, Jiahui Huang, and Konrad Schindler Andreas Wieser. Dynamic 3D Scene Analysis by Point Cloud Accumulation. In *European Conference on Computer Vision, ECCV*, 2022.

Zhao Jin, Yinjie Lei, Naveed Akhtar, Haifeng Li, and Munawar Hayat. Deformation and Correspondence Aware Unsupervised Synthetic-to-Real Scene Flow Estimation for Point Clouds. In *IEEE Conf. Comput. Vis. Pattern Recog.*, pp. 7233–7243, 2022.

Philipp Jund, Chris Sweeney, Nichola Abdo, Zhifeng Chen, and Jonathon Shlens. Scalable Scene Flow From Point Clouds in the Real World. *IEEE Robotics and Automation Letters*, 12 2021.

<sup>3</sup>Links to these materials will be provided after review.

Diederik P Kingma and Jimmy Ba. Adam: A method for stochastic optimization. *arXiv preprint arXiv:1412.6980*, 2014.

Yair Kittenplon, Yonina C Eldar, and Dan Raviv. Flowstep3d: Model unrolling for self-supervised scene flow estimation. In *IEEE Conf. Comput. Vis. Pattern Recog.*, pp. 4114–4123, 2021.

Alex Lang, Sourabh Vora, Holger Caesar, Lubing Zhou, Jiong Yang, and Oscar Beijbom. PointPillars: Fast Encoders for Object Detection From Point Clouds. In *Proceedings of the 2019 IEEE/CVF Conference on Computer Vision and Pattern Recognition (CVPR)*, pp. 12689–12697, 2019.

Mengtian Li, Yu-Xiong Wang, and Deva Ramanan. Towards streaming perception. In *Computer Vision–ECCV 2020: 16th European Conference, Glasgow, UK, August 23–28, 2020, Proceedings, Part II 16*, pp. 473–488. Springer, 2020.

Ruibo Li, Guosheng Lin, Tong He, Fayao Liu, and Chunhua Shen. HCRF-Flow: Scene flow from point clouds with continuous high-order CRFs and position-aware flow embedding. In *IEEE Conf. Comput. Vis. Pattern Recog.*, pp. 364–373, 2021a.

Ruibo Li, Chi Zhang, Guosheng Lin, Zhe Wang, and Chunhua Shen. RigidFlow: Self-Supervised Scene Flow Learning on Point Clouds by Local Rigidity Prior. In *IEEE Conf. Comput. Vis. Pattern Recog.*, pp. 16959–16968, 2022.

Xueqian Li, Jhony Kaezemel Pontes, and Simon Lucey. Neural Scene Flow Prior. *Advances in Neural Information Processing Systems*, 34, 2021b.

Xingyu Liu, Charles R Qi, and Leonidas J Guibas. FlowNet3D: Learning Scene Flow in 3D Point Clouds. *Proceedings of the IEEE/CVF Conference on Computer Vision and Pattern Recognition (CVPR)*, 2019.

Nikola Lopac, Irena Jurdana, Adrian Brnelić, and Tomislav Krljan. Application of Laser Systems for Detection and Ranging in the Modern Road Transportation and Maritime Sector. *Sensors*, 22(16), 2022. ISSN 1424-8220.

Himangi Mittal, Brian Okorn, and David Held. Just Go With the Flow: Self-Supervised Scene Flow Estimation. In *IEEE Conf. Comput. Vis. Pattern Recog.*, June 2020.

Mahyar Najibi, Jingwei Ji, Yin Zhou, Charles R. Qi, Xinchen Yan, Scott Ettinger, and Dragomir Anguelov. Motion Inspired Unsupervised Perception and Prediction in Autonomous Driving. *European Conference on Computer Vision (ECCV)*, 2022.

Neehar Peri, Mengtian Li, Benjamin Wilson, Yu-Xiong Wang, James Hays, and Deva Ramanan. An empirical analysis of range for 3d object detection. *arXiv preprint arXiv:2308.04054*, 2023.

Jhony Kaezemel Pontes, James Hays, and Simon Lucey. Scene flow from point clouds with or without learning. In *Int. Conf. 3D Vis.*, pp. 261–270. IEEE, 2020.

Gilles Puy, Alexandre Boulch, and Renaud Marlet. Flot: Scene flow on point clouds guided by optimal transport. In *Eur. Conf. Comput. Vis.*, pp. 527–544. Springer, 2020.

Alec Radford, Karthik Narasimhan, Tim Salimans, and Ilya Sutskever. Improving language understanding by generative pre-training. 2018.

Pei Sun, Henrik Kretzschmar, Xerxes Dotiwalla, Aurelien Chouard, Vijaysai Patnaik, Paul Tsui, James Guo, Yin Zhou, Yuning Chai, Benjamin Caine, Vijay Vasudevan, Wei Han, Jiquan Ngiam, Hang Zhao, Aleksei Timofeev, Scott Ettinger, Maxim Krivokon, Amy Gao, Aditya Joshi, Yu Zhang, Jonathon Shlens, Zhifeng Chen, and Dragomir Anguelov. Scalability in Perception for Autonomous Driving: Waymo Open Dataset. In *Proceedings of the IEEE/CVF Conference on Computer Vision and Pattern Recognition (CVPR)*, June 2020.

Rich Sutton. The Bitter Lesson. <http://www.incompleteideas.net/IncIdeas/BitterLesson.html>, 2019.

Ivan Tishchenko, Sandro Lombardi, Martin R Oswald, and Marc Pollefeys. Self-supervised learning of non-rigid residual flow and ego-motion. In *Int. Conf. 3D Vis.*, pp. 150–159. IEEE, 2020.

Kyle Vedder and Eric Eaton. Sparse PointPillars: Maintaining and Exploiting Input Sparsity to Improve Runtime on Embedded Systems. *International Conference on Intelligent Robots and Systems (IROS)*, 2022.

*Velodyne Lidar Alpha Prime*. Velodyne Lidar, 11 2019.

Jun Wang, Xiaolong Li, Alan Sullivan, Lynn Abbott, and Siheng Chen. PointMotionNet: Point-Wise Motion Learning for Large-Scale LiDAR Point Clouds Sequences. In *2022 IEEE/CVF Conference on Computer Vision and Pattern Recognition Workshops (CVPRW)*, pp. 4418–4427, 2022.

Xinshuo Weng, Jianren Wang, Sergey Levine, Kris Kitani, and Nicholas Rhinehart. Inverting the pose forecasting pipeline with spf2: Sequential pointcloud forecasting for sequential pose forecasting. In *Conference on robot learning*, pp. 11–20. PMLR, 2021.

Benjamin Wilson, William Qi, Tanmay Agarwal, John Lambert, Jagjeet Singh, Siddhesh Khandelwal, Bowen Pan, Ratnesh Kumar, Andrew Hartnett, Jhony Kaesemeyer Pontes, Deva Ramanan, Peter Carr, and James Hays. Argoverse 2: Next Generation Datasets for Self-driving Perception and Forecasting. In *Proceedings of the Neural Information Processing Systems Track on Datasets and Benchmarks (NeurIPS Datasets and Benchmarks 2021)*, 2021.

Wenxuan Wu, Zhi Yuan Wang, Zhiwen Li, Wei Liu, and Li Fuxin. Pointpwc-net: Cost volume on point clouds for (self-) supervised scene flow estimation. In *Eur. Conf. Comput. Vis.*, pp. 88–107. Springer, 2020.

Guangyao Zhai, Xin Kong, Jinhao Cui, Yong Liu, and Zhen Yang. FlowMOT: 3D Multi-Object Tracking by Scene Flow Association. *ArXiv*, abs/2012.07541, 2020.

## A ARGOVERSE 2 AND WAYMO OPEN DATASET CONFIGURATION DETAILS

**Argoverse 2.** The Sensor dataset contains 700 training and 150 validation sequences. Each sequence contains 15 seconds of 10Hz point clouds collected using two Velodyne VLP-32s mounted on the roof of a car. As part of the training protocol for ZeroFlow, FastFlow3D, and NSFP w/ Motion Compensation, we perform ego compensation, ground point removal, and restrict all points to be within a  $102.4\text{m} \times 102.4\text{m}$  area centered around the ego vehicle, resulting in point clouds with an average of 52,871 points (Figure 6a). The point cloud  $P_{t+1}$  is centered at the origin of the ego vehicle’s coordinate system and  $P_t$  is projected into  $P_{t+1}$ ’s coordinate frame. For ZeroFlow and FastFlow3D, the PointPillars encoder uses  $0.2\text{m} \times 0.2\text{m}$  pillars, with all architectural configurations matching (Jund et al., 2021). For NSFP w/ Motion Compensation, we use the same architecture and early stopping parameters as the original method (Li et al., 2021b). For FastFlow3D and the FastFlow3D student architecture of ZeroFlow, we train to convergence (50 epochs) with an Adam (Kingma & Ba, 2014) learning rate of  $2 \times 10^{-6}$  and batch size 64. For FastFlow3D XL and the FastFlow3D XL student architecture of ZeroFlow (ZeroFlow XL 1X, ZeroFlow XL 3X), we train to convergence (10 epochs) with the same optimizer settings and a batch size 12. For ZeroFlow 3X and and ZeroFlow XL 3X, we train on an additional 240,000 unlabeled frame pairs (roughly twice the size as the Argoverse 2 Sensor train dataset), constructed by selecting 12 frame pairs at uniform intervals from the 20,000 sequences of the Argoverse 2 LiDAR dataset. For all other methods in Table 1, we use the implementations provided by Chodosh et al. (2023), which follow ground removal and ego compensation protocols from their respective papers.

**Waymo Open.** The dataset contains 798 training and 202 validation sequences. Each sequence contains 20 seconds of 10Hz point clouds collected using a custom LiDAR mounted on the roof of a car. We use the same preprocessing and training configurations used on Argoverse 2; after ego motion compensation and ground point removal, the average point cloud has 79,327 points (Figure 6b).

As shown in Figure 6, Argoverse 2 (Wilson et al., 2021) and Waymo Open (Sun et al., 2020) are significantly larger than the 8,192 point subsampled point clouds used by prior art.

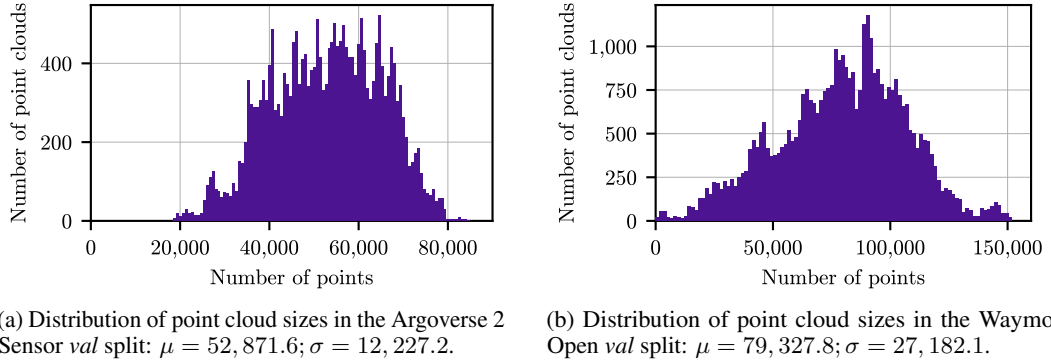


Figure 6: Point cloud size distributions for the *val* set of the Argoverse 2 Sensor (Wilson et al., 2021) and Waymo Open (Sun et al., 2020) datasets after ground removal and clipped to a  $102.4\text{m} \times 102.4\text{m}$  box around the ego vehicle.

## B EXPLORING THE IMPORTANCE OF POINT WEIGHTING

In order to train FastFlow3D using pseudo-labels, we need a replacement  $\sigma(\cdot)$  semantics scaling function described in Equation 4) because our pseudo-labels do not provide foreground / background semantics. In the main experiments, we use uniform scaling ( $\sigma(\cdot) = 1$ ).

### B.1 CAN WE DESIGN A BETTER POINT WEIGHTING FUNCTION FOR PSEUDO-LABELS?

We propose a soft weighting based on pseudo-label flow magnitude: for the point  $p$  in the pseudo-label flow  $F_{t,t+1}^*(p)$ , where  $s(p)$  represents its speed in meters per second, we linearly interpolate the

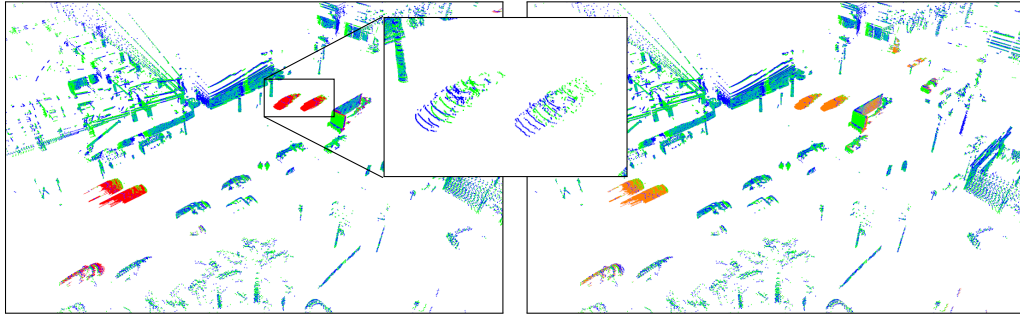


Figure 7: Scene flow estimation of two consecutive point clouds sampled 100 ms apart (green and blue, respectively) on Argoverse 2 (Wilson et al., 2021). **Left:** Ground truth scene flow annotations in red. These annotations are derived from the motion of amodal bounding boxes. **Right:** ZeroFlow’s scene flow estimates in orange, which closely match with the ground truth.

weight of  $p$  between  $0.1 \times$  at 0.4 m/s and full weight at 1.0 m/s, i.e.

$$\sigma(p) = \begin{cases} 0.1 & \text{if } s(p) < 0.4 \text{ m/s} \\ 1.0 & \text{if } s(p) > 1.0 \text{ m/s} \\ 1.8s - 0.8 & \text{o.w.} \end{cases} \quad (6)$$

These thresholds are selected to down-weight approximately 80% of points by  $0.1 \times$ , with the other 20% of points split between the soft and full weight region<sup>4</sup>. In Table 5, we show that our weighting scheme provides non-trivial improvements over uniform weighting (i.e.  $\sigma(\cdot) = 1$ ) for ZeroFlow 1X; however, it actually hurts performance for ZeroFlow 3X.

Table 5: Comparison between ZeroFlow trained on Argoverse 2 using NSFP pseudo-labels and ZeroFlow using Chodosh et al. (2023) pseudo-labels using both uniform and speed scaled point weighting. Methods with an \* have performance averaged over 3 training runs (see Supplemental C for details).

	Threeway EPE	Dynamic FG EPE	Static FG EPE	Static BG EPE	Dynamic AccRelax	Dynamic AccStrict
ZeroFlow 1X (Equation 6, NSFP pseudo-labels)*	0.087	0.217	0.023	0.023	0.394	0.164
ZeroFlow 1X (Equation 6, Chodosh et al. (2023) pseudo-labels)	0.088	0.227	0.019	0.019	0.366	0.139
ZeroFlow 1X (NSFP pseudo-labels)*	0.092	0.231	0.022	0.022	0.380	0.150
ZeroFlow 1X (Chodosh et al. (2023) pseudo-labels)	0.090	0.234	0.018	0.018	0.364	0.136
ZeroFlow XL 3X	0.056	0.131	0.018	0.018	0.595	0.305
ZeroFlow XL 3X (Equation 6)	0.058	0.139	0.017	0.017	0.574	0.286

## B.2 HOW MUCH OF FASTFLOW3D’S PERFORMANCE IS DUE TO ITS SEMANTIC POINT WEIGHTING?

Unlike ZeroFlow, FastFlow3D *can* use human foreground / background point labels to upweight the flow importance of foreground points (Section 3.3, Equation 4). To understand the impact of this weighting, we train FastFlow3D with two modified losses; rather than scaling using semantics as described in Equation 4, we uniformly weight all points ( $\sigma(\cdot) = 1$ ) or our speed based weighting (Equation 6).

As shown in Table 6, the performance of FastFlow3D ( $\sigma(\cdot) = 1$ ) and (Equation 6) degrades almost completely to ZeroFlow’s performance (e.g. 0.076  $\rightarrow$  0.085, 0.084 vs 0.087 for Threeway EPE).

This raises the question: why is the performance improvement of semantic weighting larger than the improvement of our unsupervised moving point weighting scheme (Supplemental B.1)? We

<sup>4</sup>For Argoverse 2, exactly 78.1% of points are downweighted, 11.8% lie in the soft-weight region, and 10.1% lie in the full weight region; for Waymo Open 80.0% of points are downweighted, 7.9% lie in the soft-weight region, and 12.1% lie in the full-weight region respectively.

Table 6: Comparison between ZeroFlow, FastFlow3D, and the ablated FastFlow3D with uniform scaling ( $\sigma(\cdot) = 1$ ) trained on Argoverse 2. The performance of FastFlow3D with Uniform Scaling and our speed scaling (Equation 6) are nearly identical to ZeroFlow’s performance. Methods with an \* have performance averaged over 3 training runs (see Supplemental C for details). Underlined methods require human supervision.

	Threeway EPE	Dynamic FG EPE	Static FG EPE	Static BG EPE	Dynamic AccRelax	Dynamic AccStrict
ZeroFlow 1X* (Ours)	0.087	0.217	0.023	0.023	0.394	0.164
FastFlow3D ( $\sigma(\cdot) = 1$ )	0.085	0.220	0.018	0.018	0.434	0.182
FastFlow3D (Equation 6)	0.084	0.211	0.020	0.020	0.441	0.189
FastFlow3D* (Jund et al., 2021)	0.076	0.186	0.021	0.021	0.474	0.200

conjecture that not only does semantic weighting provide increased loss on moving objects, it implicitly teaches the network to recognize the structure of objects themselves. For example, with Equation 4 scaling, end-point error on a stationary pedestrian is significantly higher than static background points, incentivizing the network to learn to detect the point *structure* common to pedestrians, even if immobile, to perfect the predictions on those points.

## C CHARACTERIZING INTER-TRAINING RUN FINAL PERFORMANCE VARIANCE FOR ZEROFLOW AND FASTFLOW3D

On Argoverse 2, Threeway EPE difference between ZeroFlow and the human supervised FastFlow3D is 1.6cm (Table 1); how much of this gap can be attributed to training variance between runs? To answer this question, we train ZeroFlow and FastFlow3D from scratch 3 times each. ZeroFlow is trained on the same Argoverse 2 NSFP pseudo-labels (Table 8), resulting in a mean Threeway EPE of 0.092m with error of 0.003m (0.3cm) in either direction, and FastFlow3D is trained on the Argoverse 2 human labels (Table 9), resulting in a mean Threeway EPE of 0.092m with error under 0.003m (0.3cm) in either direction.

To contextualize the scale of this variance, the underlying Velodyne VLP-32 sensors used to collect the Argoverse 2 are only certified to  $\pm 3$  cm of error (Lopac et al., 2022) (an order of magnitude greater than the deviation from the mean train performance for ZeroFlow), and this entirely neglects additional sources of noise introduced from other real world effects such as empirical ego motion compensation.

Table 7: Performance of ZeroFlow over 3 train runs on the same NSFP pseudo-labels.

	Threeway EPE	Dynamic FG EPE	Static FG EPE	Static BG EPE	Dynamic AccRelax	Dynamic AccStrict
ZeroFlow 1X Run #1	0.087	0.214	0.023	0.023	0.409	0.180
ZeroFlow 1X Run #2	0.087	0.215	0.024	0.024	0.397	0.164
ZeroFlow 1X Run #3	0.089	0.222	0.022	0.022	0.377	0.147
ZeroFlow 1X Average	0.087	0.217	0.023	0.023	0.394	0.164

Table 8: Performance of ZeroFlow ablated with uniform point scaling ( $\sigma(\cdot) = 1$ ) over 3 train runs on the same NSFP pseudo-labels.

	Threeway EPE	Dynamic FG EPE	Static FG EPE	Static BG EPE	Dynamic AccRelax	Dynamic AccStrict
ZeroFlow 1X ( $\sigma(\cdot) = 1$ ) Run #1	0.089	0.224	0.021	0.021	0.388	0.151
ZeroFlow 1X ( $\sigma(\cdot) = 1$ ) Run #2	0.092	0.231	0.022	0.022	0.377	0.155
ZeroFlow 1X ( $\sigma(\cdot) = 1$ ) Run #3	0.095	0.240	0.023	0.023	0.375	0.144
ZeroFlow 1X ( $\sigma(\cdot) = 1$ ) Average	0.092	0.231	0.022	0.022	0.380	0.150

Table 9: Performance of FastFlow3D over 3 train runs on the Argoverse 2 human labels.

	Threeway EPE	Dynamic FG EPE	Static FG EPE	Static BG EPE	Dynamic AccRelax	Dynamic AccStrict
FastFlow3D Run #1	0.074	0.181	0.020	0.020	0.462	0.190
FastFlow3D Run #2	0.076	0.186	0.021	0.021	0.480	0.209
FastFlow3D Run #3	0.079	0.191	0.023	0.023	0.481	0.203
FastFlow3D Average	0.076	0.186	0.021	0.021	0.474	0.200

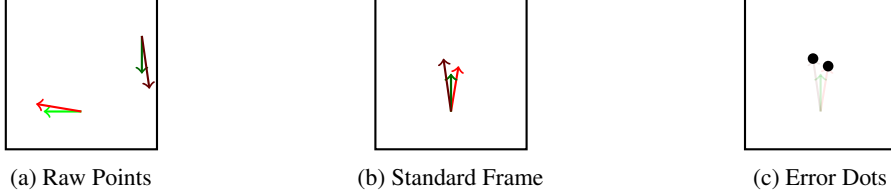


Figure 8: Process for constructing the endpoint residual plots. The raw points (Figure 8a) are transformed into a standard frame with the ground truth vector pointing up and the endpoint at the center of the plot (Figure 8b), and the residual endpoints are accumulated (Figure 8c).

## D ESTIMATING HUMAN LABELING VERSUS PSEUDO-LABELING COSTS

NSFP pseudolabeling of the Argoverse 2 train split (700 sequences of 150 frames) required a total of 753 hours of NVidia Turing generation GPU time. At September, 2023 Amazon Web Services EC2 prices, a single g4dn.xlarge, equipped with a single NVidia Tesla T4, costs \$0.526 per hour<sup>5</sup>, for a total cost of \$394 to pseudo-label. By comparison, at an estimated \$0.10 per frame per cuboid (no public cost statements exist for production quality AV dataset labels, but this is the standard price point within the industry), Argoverse 2’s train split has an average of 75 cuboids per frame (Wilson et al., 2021), for a total cost on the order of \$787,500 to human annotate.

## E DETAILS ON ENDPOINT RESIDUALS

The process of constructing these endpoint residual plots is shown in Figure 8. For moving points (points with a ground truth flow vector magnitude  $>0.5\text{m/s}$ ), the raw points (Figure 8a) are transformed into a standard frame with the ground truth vector pointing up and the endpoint at the center of the plot (Figure 8b), and the residual endpoints are accumulated (Figure 8c).

<sup>5</sup><https://aws.amazon.com/ec2/pricing/on-demand/>

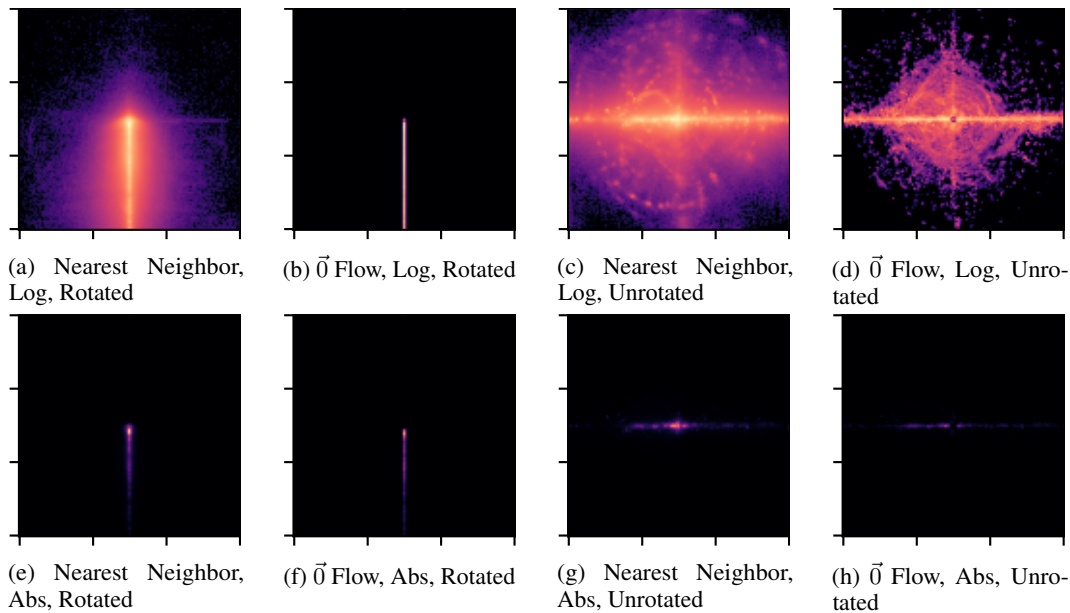


Figure 9: Birds-eye-view heatmap of endpoint residuals for naïve flow methods of predicting flow (Nearest Neighbor and  $\vec{0}$  Flow on all points) for non-background points moving above 0.5m/s in the raw coordinate frame of the ground truth labels. Brighter color indicates more points in each bin. Perfect labels would produce a single central dot. Distance between ticks is 1 meter. Top row shows frequency on a log color scale to display error distribution shape. Bottom row shows frequency on an absolute color scale to display centroid. Left half shows results in the rotated coordinate frame of the ground truth labels. Right half shows results in the unrotated coordinate frame of the ground truth labels.